Investigating the effect of Aluminum dopping on the structural, optical, electrical, and sensing properties of ZnO films

Zainab T. Hussain[1], Wasna'a M. Abdulridha[2], Ashwaq A. Jabor[3], Julfikar Haider[4]

[1]*Directorate of Materials Research, Ministry of Science and Technology, Baghdad, Iraq*

[2]*Basic Science Department, College of Dentistry, University of Kufa, Najaf, Iraq*

[3]*Department of Materials Research, Ministry of Science and Technology, Baghdad, Iraq*

[4]*Department of Engineering, Manchester Metropolitan University, Manchester, UK*

Corresponding Author

Dr Wasna'a M. Abdulridha

Basic Science Department

College of Dentistry

University of Kufa, Najaf

Iraq

Email:wasnaa.albaghdadi@uokufa.edu.iq

Abstract

More recently aluminum doped zinc oxide (ZnO:Al) thin films have attracted a lot of attention as an alternative to indium tin oxide (ITO) for optoelectronic devices in order to produce energy such as solar cells. In this work, ZnO:Al thin films were deposited onto quartz and silicon substrates by RF magnetron sputtering technique and the effect of Al doping on structural, optical and sensing properties of the films were studied. The dopant concentration was varied between 1 wt.% and 3 wt.% in the thin films. The crystalline structure of the films were investigated by X-ray diffraction, which indicated wurtzite structure along (100) plane. The surface morphology of the films characterized by AFM revealed that the grain size decreased with increasing dopant concentration. The films also exhibited changes in optical properties due to a decrease in band gap with increasing Al concentration. Hall measurement confirmed that the ZnO films exhibited an n-type conductivity. The results of gas sensing experiments showed that the sensitivity of the ZnO films for detecting CO_2 enhanced with an increase in dopant concentration.

Keywords

Transparent conductive oxides (TCO), Zinc oxide, Aluminum, Gas Sensor, Magnetron sputtering

1. Introduction

Transparent conductive oxide (TCO) films such as ZnO_2, SnO_2, CdO, and In_2O_3 are widely used in a variety of semiconductor devices due to their wide optical band gap, high stability against heat, high electrical conductivity (exhibiting a low resistivity of roughly 10^{-3} to 10^{-4} Ω.cm) and high transparency (about 80% in the visible region) [1, 2]. More recently, zinc oxide (ZnO) has attracted a lot of attention as an important TCO material for sensor applications due to its direct energy band gap (3.4 eV), large exciton binding energy (60 meV), capable of absorbing UV radiation, good transparency with high electron mobility, and wrutzite structure [3, 4]. ZnO is widely used in various applications such as transistors, piezoelectric devices, and solar cell electrodes [5]. Owing to its well-known surface conductivity, ZnO is sensitive to many gases such as CO [6], O_2[7],CH_4[*8], NO_2[9, 10], ethanol [11] and ammonia [12*] making it suitbale for fabricating gas sensors. To deposit Zinc oxide thin films, several techniques have been employed such as chemical vapor deposition [13], photocatalyst, pulse laser ablation in liquid [14], sol-gel process [15], spray pyrolysis [1, 16] and magnetron sputtering [3, 17, 18]. Among the techniques, magnetron sputtering is most commonly used due to its key advantages such as high deposition rate, very good surface uniformity, good structural integrity, good adhesion to substrate, easily controllable film thickness and film properties by adjusting certain process parameters, and scalable to large area film for industrial applications [19, 20].

The electrical properties of intrinsic ZnO are limited due to the lack of free carriers [21]. Therefore, metal dopants can be incorporated in the ZnO films to increase the free carriers in order to improve its electrical and gas sensing properties. Some of the common N-type doping elements include aluminium (Al), gallium (Ga) and titanium (Ti) [3, 4, 9, 12]. The introduced N-type donor atoms contribute to one extra electron in the ZnO lattice, which increases the film conductivity [22].

A number of studies have been carried out to enhance the gas sensing properties of ZnO such as changing the nanostructures, elemental doping and formation of heterostructures by different type of metal oxides. However, doping ZnO films with Al can produce defects, which can promote conductivity of the films suitable for developing gas sensor for hazardous and explosive gas ambients [9, 22]. For this purpose, the combination of Al and ZnO attracted significant interest

owing to their availability at low cost, non- toxic, good stability in hydrogen, cheaper and easy manipulation of electrical and optical properties [23, 24].

After extensive literature survey, it was found that even though Al doped ZnO films were studied for fundamental film characterisations and several gas sensing performance, but to the author's best knowledge CO_2 gas sensing studies by this type of films are limited. Therefore, in this study, the effect of Al doping on the morphological, structural, optical properties and electrical properties of ZnO thin films deposited by RF magnetron sputtering was systematically studied. Furthermore, the sutiability of the doped films as a gas sensor was evaluated by measuring the sensing properties in the presence of CO_2 gas.

2. Experimental procedure

2.1. Materials

Aluminum (Al) doped zinc oxide thin films were deposited onto a glass substrate. Zinc oxide (99.99% purity) dopped with different concentrations (0 wt.%, 1 wt.% and 3 wt.%) of Al powder (99.99% purity) was obtained as the film materials. 1 wt% and 3 wt% Al powders were mixed with 99 wt% and 97 wt% ZnO powders respectively to prepare composite pallets as the target materials for the RF sputtering. The ZnO pallets were also prepared as the target material for pure ZnO film deposition. The pallets were 50 mm in diameter and 5 mm in height. A high-purity argon (99.999%) was used as the operating gas.

2.2. Coating deposition method

The transparent conductive ZnO:Al films were deposited on a square (2.5×2.5 cm^2) glass substrate by RF magnetron sputtering. The magnetron sputtering chamber was made from stainless steel in the form of a cylinder with 250 mm in height and 230 mm in diameter as shown in Figure 1. The substrate was fixed parallel to the target surface on a rotating planetary sample-holder (100 mm in diameter) with tunable substrate-target distance. The distance between the ZnO:Al target and substrate was set to approximately 40 mm. During the deposition the sample temperature can be carefully adjusted by a digital on/off controller coupled with a thermocouple positioned near the substrate. Before the introduction in the deposition chamber, the glass substrate was ultrasonically cleaned in acetone, ethanol and deionized water. Immediately after cleaning, the

substrate was loaded into the sputtering chamber. Then the chamber was evacuated to a base pressure of 5.5×10^{-6} mbar and the argon gas was introduced into the chamber. A pre-sputtering process was carried out at a pressure of 1.5×10^{-3} mbar in order to clean the target surface and ensure stabilized sputtering conditions. Thin films were obtained after fixing the substrate temperature to 80 ± 5 ^{o}C. The working RF power (P_W) and pressure (P_{ar}) were varied in the ranges of 15 - 50 mW.mm^{-2} and 1.5×10^{-3} - 5.1×10^{-3} mbar respectively. Although the film can be deposited on to the substrate either in static mode or in dynamic rotating mode, static mode was used in this investigation. No further post-treatment on the films was applied. The films on glass susbtrate were used for Atomic Force Microscopy (AFM) and gas sensing test. However, the films were deposited on quartz substrate for optical property measurement. Furthermore, electrical property of the film was measured after depositing on a p type Si substrate.

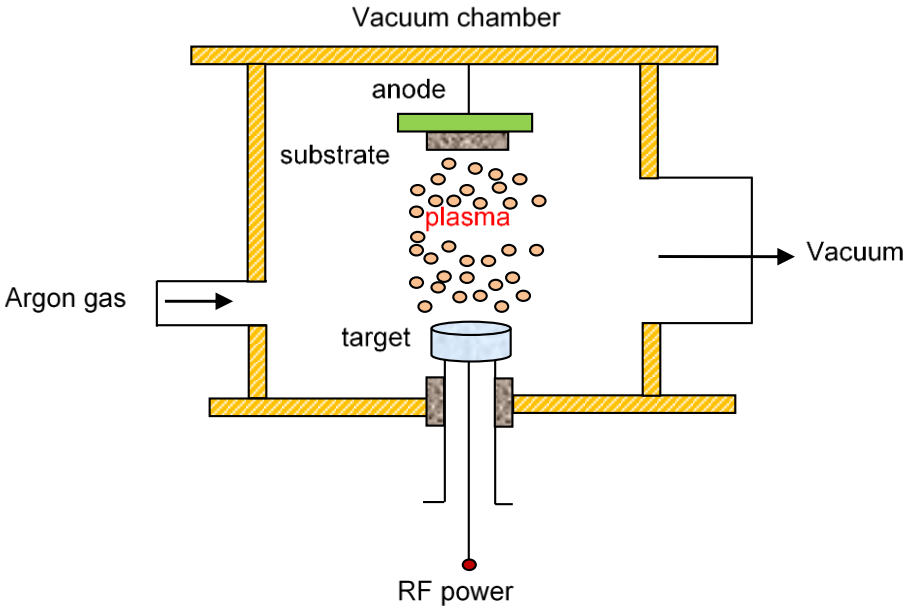

Figure 1. RF magnetron sputtering deposition chamber for the deposition of ZnO:Al thin films.

2.3. Characterization techniques

The crystalline structure and orientation of the ZnO:Al thin films were determined by X-ray diffraction (XRD) technique using a Shimadzu-XRD 6000 (Shimadzu Company, Japan) diffractometer with a BraggBrentano geometry and employing a CuKα source (40 kV, 30 mA) at

an incident angle of 2°. The average crystallite dimensions were estimated by the Scherrer formula (equation 1) [25].

$$t = \frac{k\lambda}{[\beta \cos(\theta)]} \quad (1)$$

where k is the shape factor (usually 0.9), λ is the X-ray wavelength, θ is the Bragg diffraction angle, β is the full width at half maximum (FWHM) in radians.

Surface morphology of the ZnO:Al film was investigated using an AFM. The film thickness was determined by a KLA - Tencor Stylus Profiler P10. UV-VIS-NIR spectrophotometer (Shimadzu-3600, Japan) was used for characterizing transmittance of the film in the wavelength range of 200 to 1100 nm. Equation 2 was used to calculate the absorbance.

$$A = 100 - R - T \quad (2)$$

The band gap of the film were determined using Tauc's plot method [26] using equation 3.

$$(\alpha h\nu)^2 = B(h\nu - E_g) \quad (3)$$

where α is the absorption coefficient, hν is the incidentphoton energy, E_g is the optical gap energy for direct allowedtransitions and B is a constant dependent on the refractive index of the material, the electron effective mass and the speed of light in vacuum. Plotting $(\alpha h\nu)^2$ as a function of the incident energy (hν) the optical gap may be estimated by extrapolating the linear portion of the line until it intercepts the x-axis, at which point αhν = 0.

The local sheet resistances of ZnO:Al films was measured by four probe technique, using a Kuliche-Soffa head (UK) with a Keithley 220 programmable current source and a Keithley 195A digital multimeter. The sheet resistanceof the entire sample was evaluated by van der Paw technique, using a Keithley 2636 System (SourceMeter® Instruments).

All the thin film thicknesses were found in the range of 114 nm - 126 nm at 100 W target power, 30 min of deposition time and a substrate temperature of 80°C. Copper mesh mask was placed over the deposited ZnO:Al films to prepare gas sensors. Test gas (CO_2) were passed in a gas sensor

chamber through opening a relevant valve. The sensor response was defined (equation 4) as a ratio of the resistance of the sensor in dry air (R_a) to that in the target gas (R_g) at room temperature.

$$S = \frac{R_g}{R_a} \times 100 \quad (4)$$

Where S is the sensitivity (%).

3. Results and discussion

3.1. Crystalline structure

Figure 2 shows the X-ray diffraction patterns for the undoped and Al doped ZnO thin films on glass substrate at room temperature with different Al concentrations. It was observed that the ZnO film displayed a polycrystalline structure having a type of hexagonal wurtzite. The growth directions of the ZnO films along (100), (002), and (101) planes corresponded to sharp peaks at 31.6º, 34.2º, and 36.1º respectively, which agreed well with the reported standard values (JCPDS card no. 36-1451). Furthermore, the (002) peak indicated a c-axis preferred crystal orientation for the pure ZnO film. With the introduction of Al doping, the crystal orientation of the ZnO film altered with a new (100) peak shifted towards high diffraction angle and the (002) peak intensity decreased. With the increase of Al concentration at 3 wt.%, the peak further shifted towards lower diffraction angle with an additional decrease in peak intensity. The difference in ion sizes between Zn (0.074 nm) and Al (0.054 nm) generated stress within the film, which led to a shift in peak position and changed the characteristics of the peak [27, 28]. The average crystalline size of ZnO thin film was 54.8 nm and slightly decreased with the addition of 1 wt.% (45.09 nm) and 3 wt.% (42.19 nm) Al concentrations.

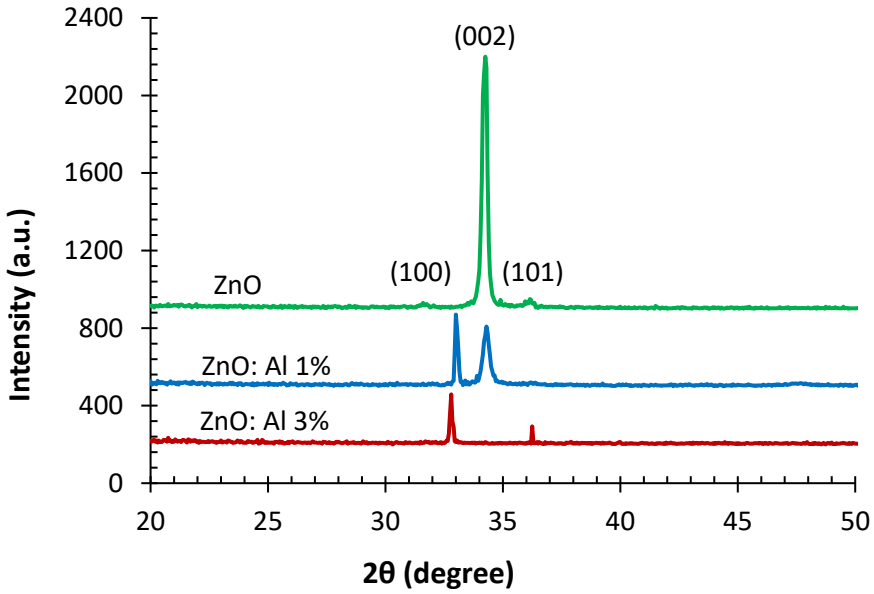

Figure 2. XRD patterns of ZnO and ZnO:Al thin films at different Al doping.

3.2. Surface morphology and grain size

Figure 3 shows 3D AFM images of the ZnO:Al thin films deposited on glass substrate at different aluminum concentrations. Figure 4 presents the particle distribution in different thin films. Although the particle sizes for all films showed normal distribution but for the ZnO film the distribution was slightly wider with higher particle sizes (40-160 nm). However, the values were slightly lower for the al dopped films (40-120 nm). The average grain size for the ZnO film (86.72 nm) slightly decreased with the addition of 1 wt.% (77.59 nm) and 3 wt.% (73.72 nm) Al concentrations (Figure 5Figure 5). These results were also consistent with the XRD observations although the values were slightly lower. Surface roughness was also decreased with the increase in doping concentration [29, 30]. The presence of Al leading to the change in morphological structure of ZnO:Al thin films could be responsible for these observations. Therefore, it was clear from the AFM results that with the addition of Al in ZnO film can reduce the grain size and surface roughness.

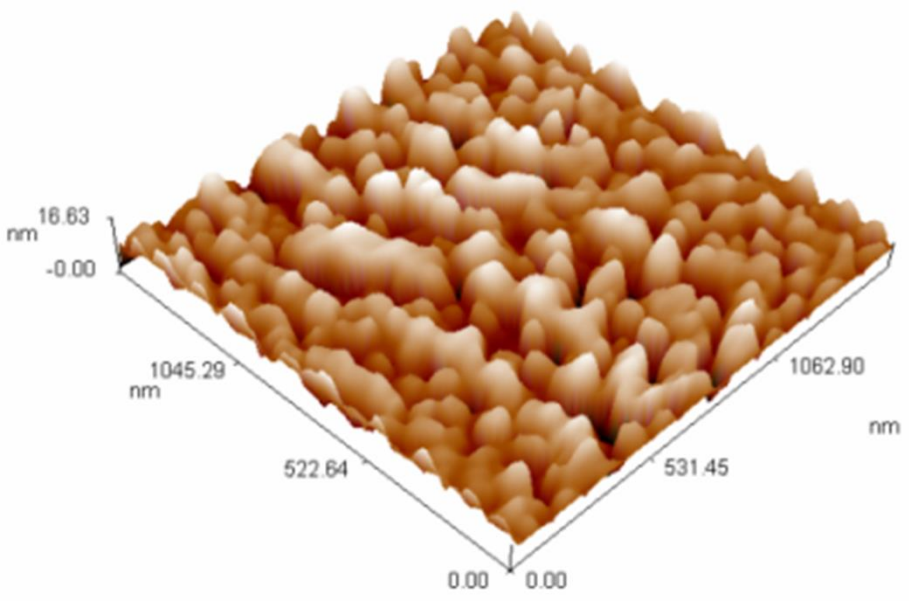
16.63
nm
-0.00
1045.29
nm
522.64
0.00
0.00
1062.90
nm
531.45

(a)

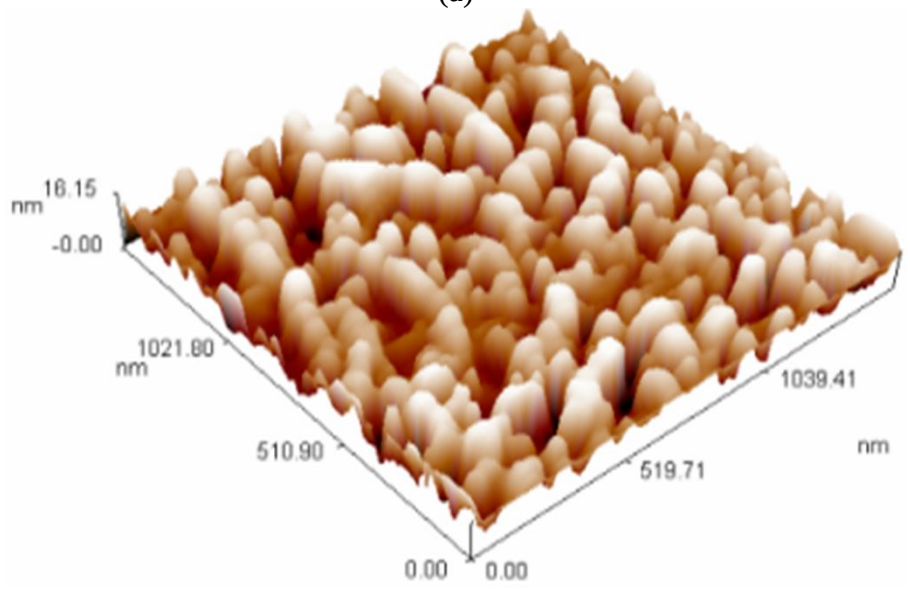
16.15
nm
-0.00
1021.80
nm
510.90
0.00
0.00
1039.41
nm
519.71

(b)

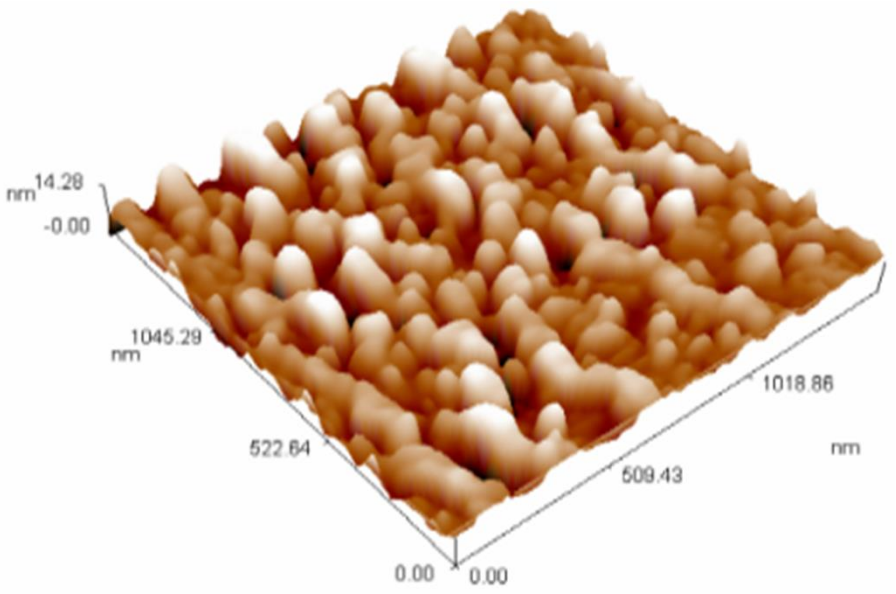

(c)

Figure 3. 3D AFM images of the ZnO:Al thin films at different aluminuim doping: (a) ZnO, (b) ZnO:Al 1 wt.% and (c) ZnO:Al 3 wt.%.

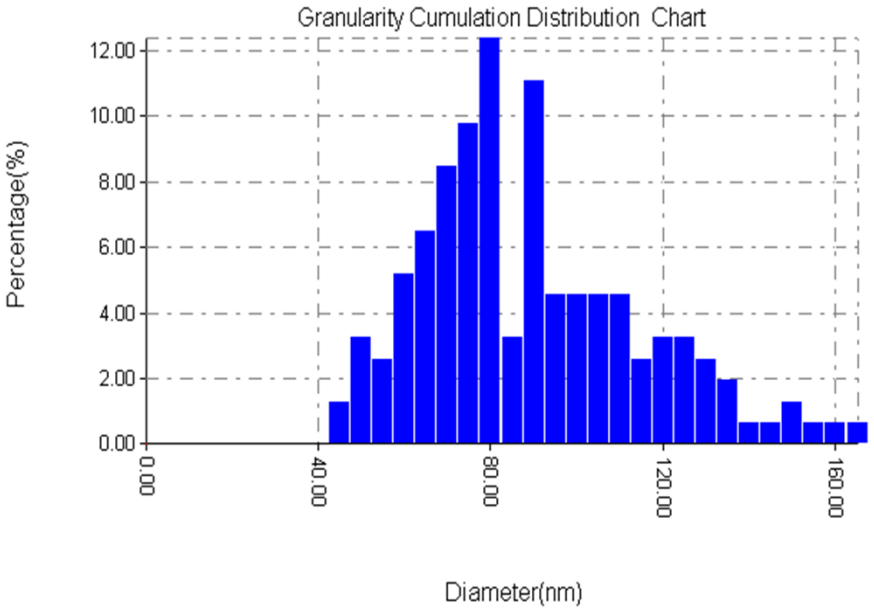

(a)

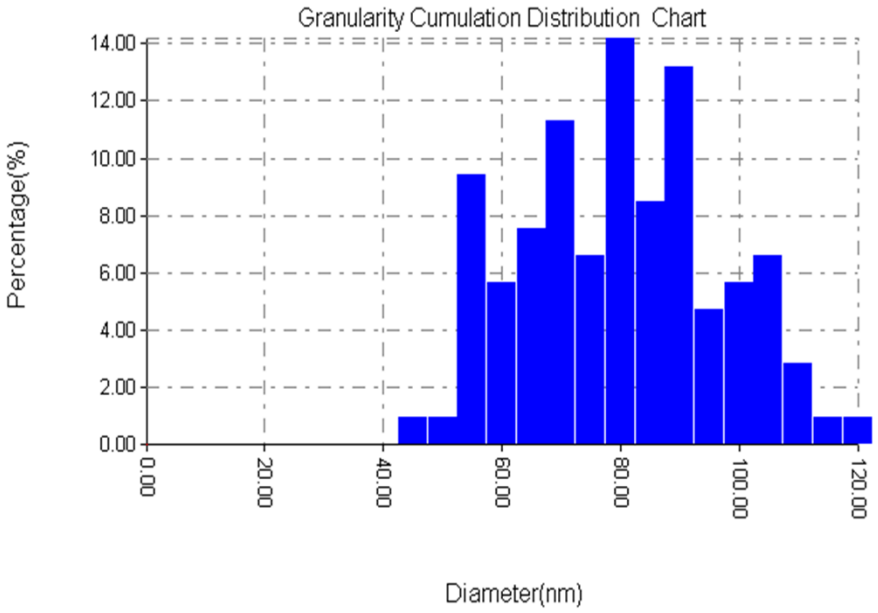

(b)

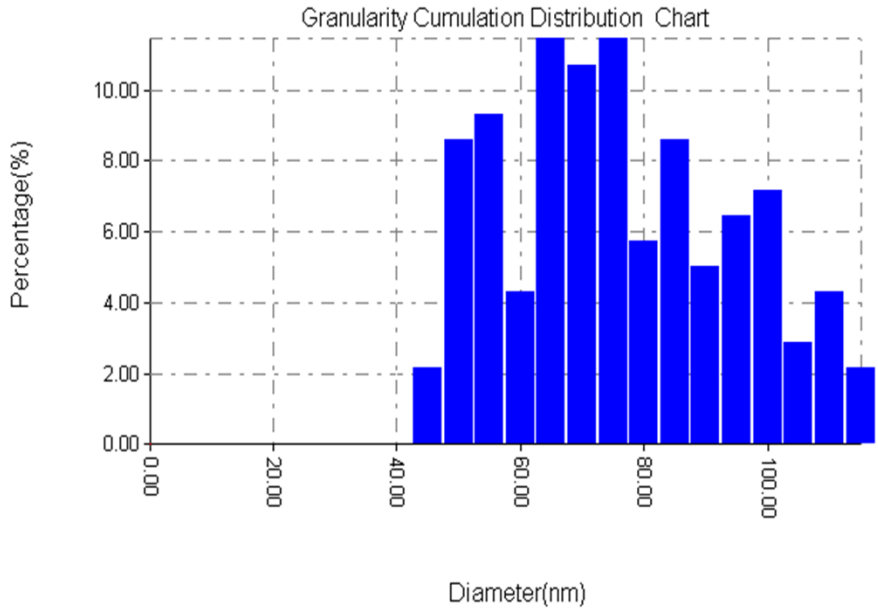

(c)

Figure 4. Granularity cumulation distribution charts for the ZnO:Al thin films at different aluminuim doping: (a) ZnO, (b) ZnO:Al 1 wt.% and (c) ZnO:Al 3 wt.%.

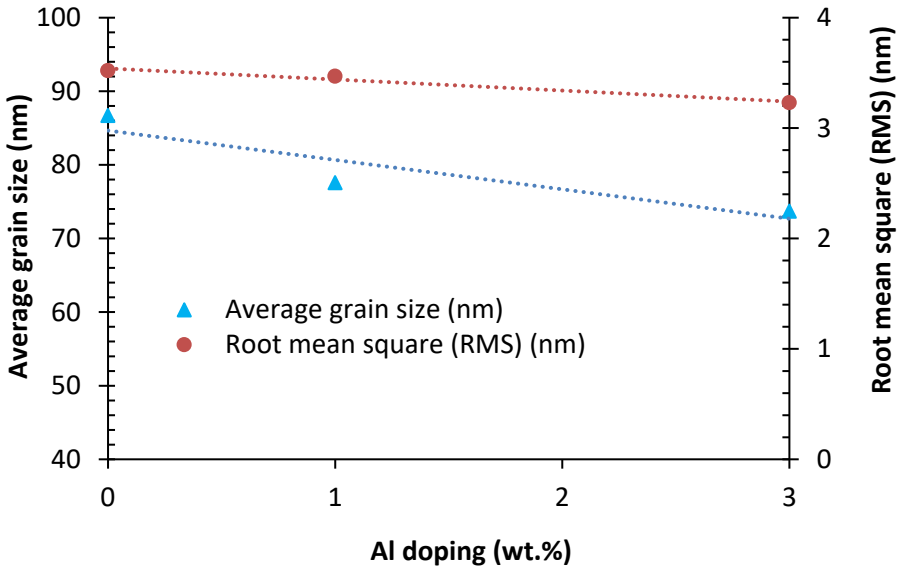

Figure 5. Average grain size, and surface roughness (root mean square, RMS) for ZnO:Al thin films at different Al dopings.

3.3. Optical properties

Transmittance as a function of wavelength in the range of 150-900 nm was measured for the ZnO:Al thin films at different Al doping concentrations as illustrated in Figure 6. The principal features of the graphs were characterized by a sharp increase in the transmittance with an increase in wavelength of light above 350–400 nm [20]. The graphs indicated that the optical transmittance spectra in the visible region was greater than 80% compared to the low transmittance of pure ZnO (27%). The results showed that the optical transmittance of the ZnO:Al thin films increased with the increase in Al concentration although the increament was only 2.5% between 1 wt% and 3 wt% Al doping [31, 32]. An opposite trend in the absorbance was found in the curves presented in Figure 7 for different films.

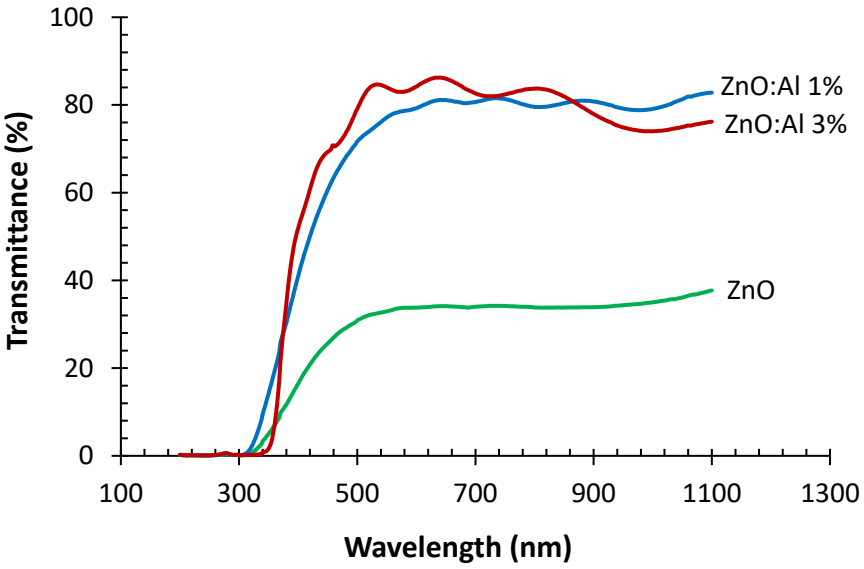

Figure 6. Transmittance of ZnO:Al films as a function of aluminuim concentration.

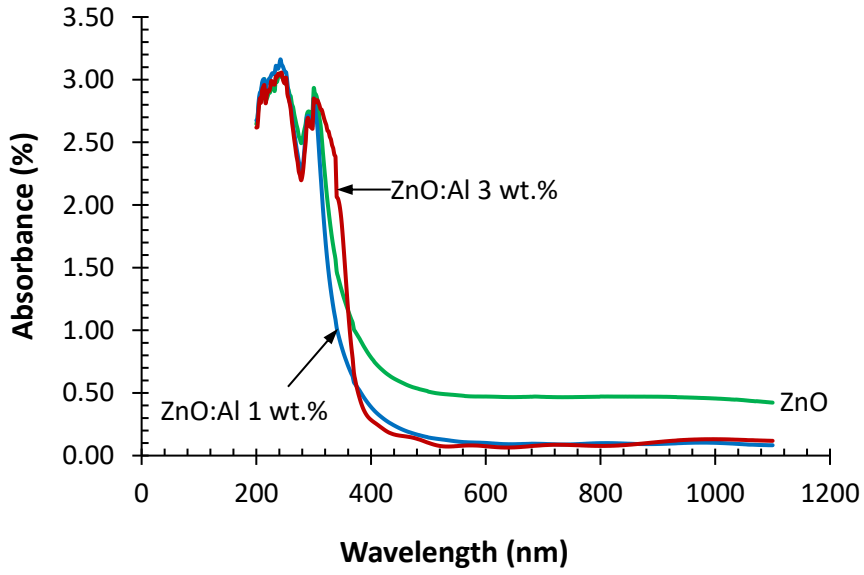

Figure 7. Absorbance of ZnO:Al films as a function of aluminuim concentration.

Figure 8 shows a linear dependence plot of (hυ) against $(\alpha h\upsilon)^2$, indicating a direct transition of ZnO:Al thin films with n-type semiconductor films [33, 34]. The band gap was determined by extrapolating the linear part of $(\alpha h\upsilon)^2$ curve intersecting at the (hυ) axis. The direct optical band gap (E_g) of pure the ZnO film (3.15 eV) increased to 3.4 eV for 3 wt.% Al doping. This results

were in good agreement with the findings presented in the literature [29, 35]. Because the state under Fermi level was occupied by electron; and at heavy doping Fermi level will enter in the conduction band [36].

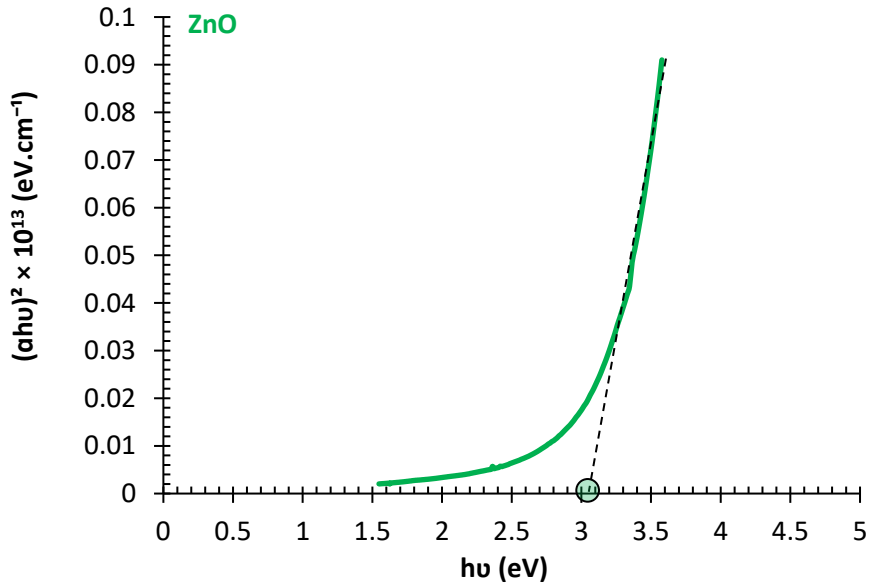

(a)

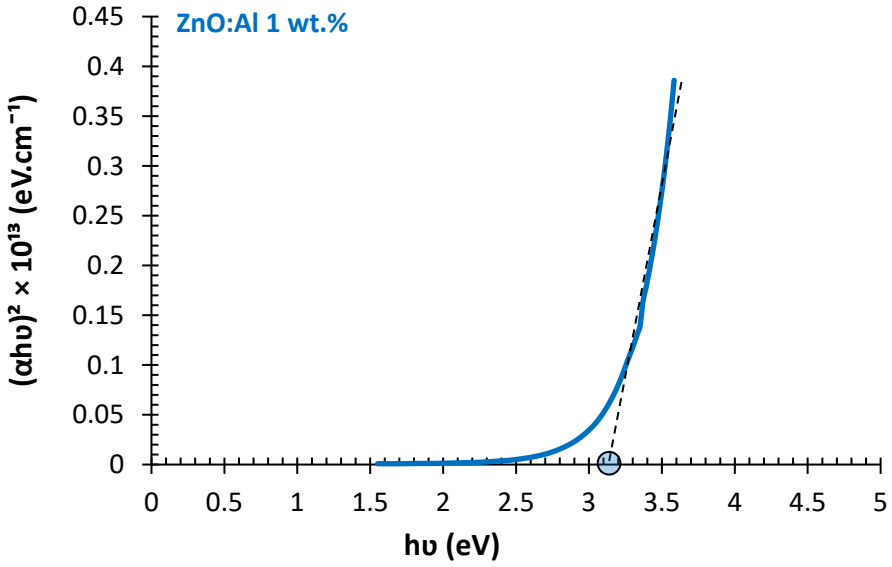

(b)

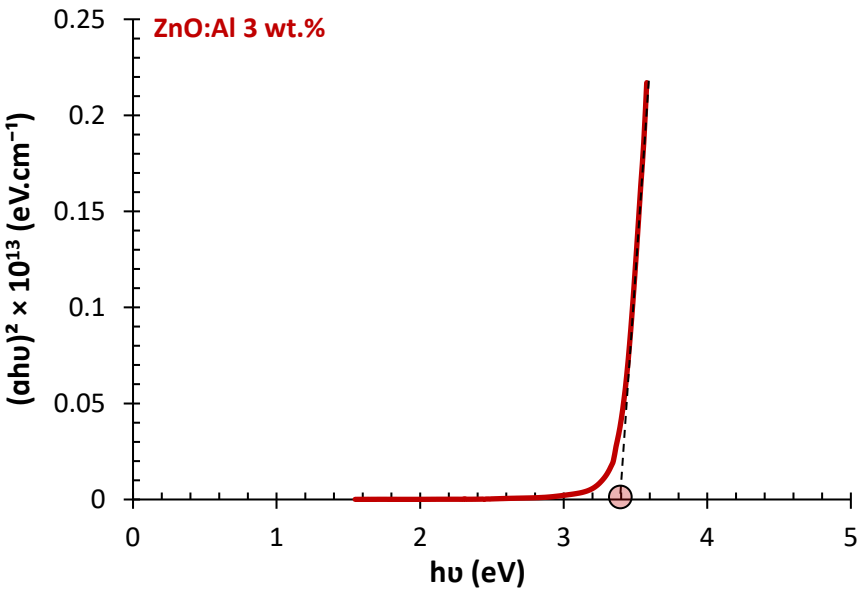

(c)

Figure 8. (ahυ)² as a function of photo energy of ZnO:Al films at different aluminium dopings: (a) ZnO, (b) ZnO:Al 1 wt.% and (c) ZnO:Al 3 wt.%.

3.4. Electrical properties

Figure 9 presents the dependency of Al concentrations on the electrical resistivity (ρ) and Hall mobility of the ZnO:Althin films. It was seen from the figure that the resistivityof the ZnO film (88.9 Ω.cm) decreased initially with an Al dopant of 1 wt.% (1.608 Ω.cm). However, with further increase in Al at 3 wt.% the resistivity value only slightly decreased to 1.46 Ω.cm. On the other hand, the mobility of the ZnO film (15.57 cm^2/Vs) increased to 73.61cm^2/Vs and 144.9 cm^2/Vs with the Al concentrations of 1 wt.% and 3 wt.%respectively. The decrease in resistivity (ρ) with the increase in Al ratio could be attributed to the increase in carrier concentration, which also led to an increase in mobility [37, 38]. The results also demonstrated that the electrical resistivity was inversely proportional to the mobility with pure ZnO film having the highest resistivity due to its low carrier concentration. During doping, host Zn sites were substituted by extrinsic Al and provided an extra electron for increasing career concentration [31].

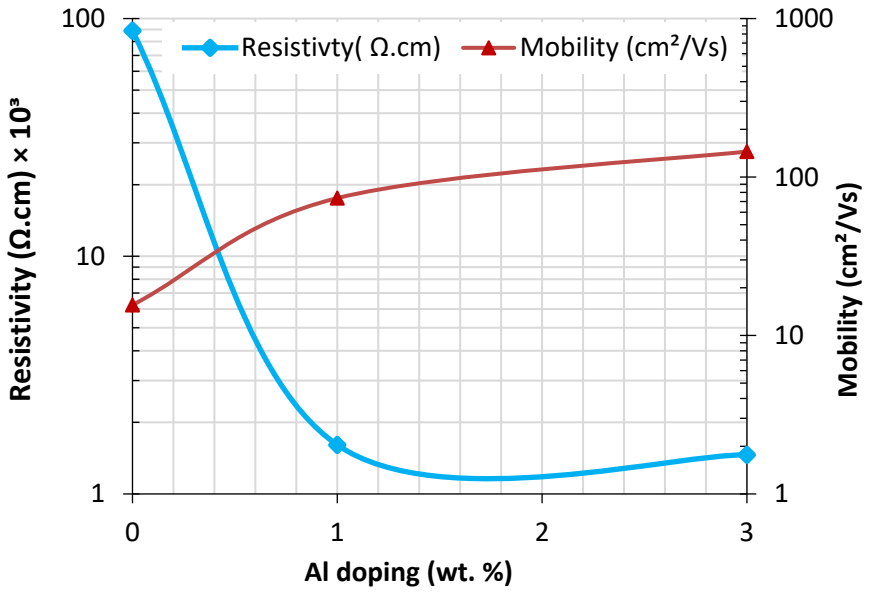

Figure 9. The resistivity and mobility for ZnO:Al films as a function of aluminium dopings.

Figure 10 shows I-V characterization of ZnO:Al deposited at various Al concentrations (0 wt.%, 1 wt.% and 3 wt.%) at room temperature indicated that the maximum values for forward currents at a bias voltage of 10 V were 3.2 mA, 5.8 mA and 9 mA respectively. Al doped thin films exhibited higher current than that of the undoped film due to the incorporation of Al at ZnO lattice. This created donor levels in optical band gap and thereby increasing the electron concentration [39, 40].

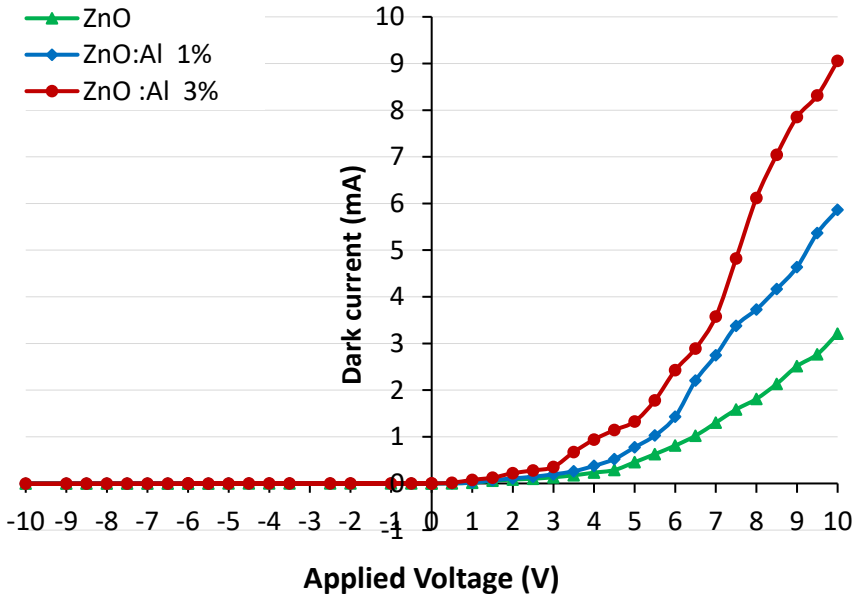

Figure 10. Dark I-V Characterization with forward and revers bias of ZnO:Al at different Al concentrations.

3.5. Gas sensing performance

Gas sensing performance of the ZnO:Al nanofilms was carried out at room temperature by recording the change in film's electrical resistance when exposed to CO_2 gas. In general, surface reactions with reducing chemical species such as gas causes an increase in the conductance of the films [41]. This electrical sensitivity of the films in coatct with gas can be used as a sensor. The sensitivity of the ZnO:Al films at different Al dopings gradually increased with the increase in time of exposure to CO_2 gas at room temperature as shown in Figure 11, which showed that the sensitivity values of the ZnO:Al samples increased by 56% - 80% in comparison with pure ZnO films approximately. In fact, for the ZnO gas sensors, Al doping caused to introduce more oxygen vacancy related defects in the nanoparticles of ZnO. Therefore, more adsorption sites for molecules of the gas provided by the oxygen vacancies resulted in a highly active surface for reaction [42]. However, after reaching the peak sensitivity, all the films showed a continuous decrease in the sensitivity possibly due to a reduction in active adsorption sites within the films.

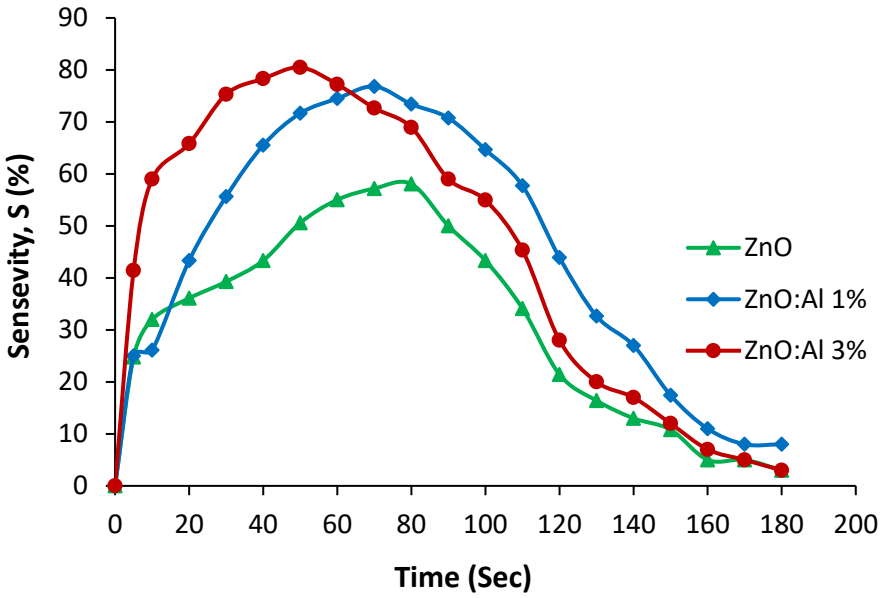

Figure 11. Sensitivity of ZnO:Al films as a gas sensor at different Al dopings.

The response time is defined as the time required for a gas sensor to achieve 90% of the maximum decrease in the electrical resistance on exposure to the gas. While the recovery time for the gas sensor is expressed as the time required to regain 90% of the maximum resistance back when exposed to clean air. The response time variations with different Al concentrations at room temperature are presented in Figure 12. It was noted that the response time decreased from 60 sec to 20 sec in contact with CO_2 gas with the increasing Al concentration from 0 wt.% to 3 wt.% respectively. This could be attributed to the increase in availability of vacant sites on thin films for gas adsorption with the increase of doping amount [43, 44].

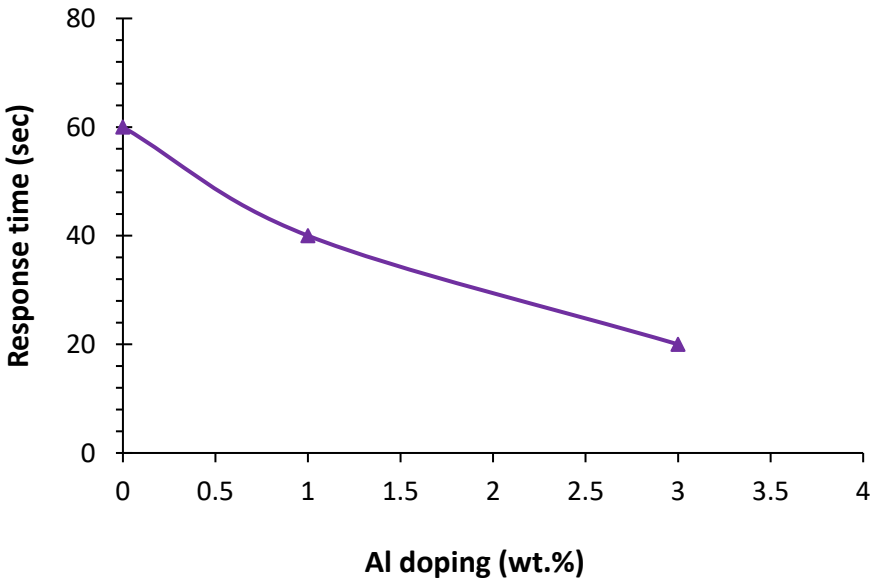

Figure 12. Response time for ZnO:Al films at different Al dopings.

4. Conclusions

This study investigated optical, structural, and electrical properties of RF magnetron sputtered zinc oxide films (ZnO:Al) doped with 1 wt.% and 3 wt.% Al. X-ray diffraction of the ZnO films showed a polycrystalline hexagonal structure and it was evident that a new (100) peak appeared with shifts to the higher diffraction angle after Al doping. AFM measurments showed that the average grain size decreased from 86.72 nm to 73.72 nm as the aluminum concentration increased. In terms of optical properties, Al doped films displayed transmittance higher than 80% in the visible region. Furthermore, an increasing trend of band gap of the film was observed with the increase of Al concentration. The improvement in electrical properties was also observed by the reduction of

restivity and increament in mobility and drak current with the increase in Al doping. Sensing characteristics of the ZnO:Al nanoscale thin films demonstrated the highest sensitivity value for CO_2 gas with 3 wt.% Al dopants. Based on the experimental characterisations, it can be concluded that the ZnO film with 3wt.% Al concentration would be suitable for optoelectronic device and gas sensing applications.

References

1. R. Sabry and D. Kafi, ZnO: Al nanostructure gas sensor by spray pyrolysis. J. Appl & Natu Sci., 2 (2013) 29-38.

2. D. Look, J. Hemsky and J. Rozdove, Residual Native Shallow Donor in ZnO. Phys. Rev. Lett., 82 (1999) 2552-2555.

3. H. Czternastek, ZnO thin films prepared by high pressure magnetron sputtering. Opto-Elec. Rev., 12 (2004) 49-52.

4. R. Ismail, S. Al-Jawad and N. Hussein, Preparation of n-ZnO/p-Si solar cells by oxidation of zinc nanoparticles: effect of oxidation temperature on the photovoltaic properties. J.Appl Phys A. 117 (2014) 1977-1984.

5. L. P. Dai, H. Deng, Y. Mao, D.Jang, The recent advances of research on p-type ZnO thin film, J. Mater. Sci. Mater. Electr.19 (2008) 727-734.

6. Chang, S. J., Hsueh, T .J., Chen, I. C., Huang, B. R., Highly sensitive ZnO nanowire CO sensors with the adsorption of Au nanoparticles. Nanotechnology, 19 (2008) 175502

7. Al-Hardan, N., Abdullah, M.J., Abdul Aziz, A.: Impedance spectroscopy of undoped and Cr-doped ZnO gas sensors under different oxygen concentrations. Appl. Surf. Sci. 257 (2011). 8993-8997

8. Hamedani, N.F., Mahjoub, A.R., Khodadadi, A.A., Mortazavi,Y.: CeO2 doped ZnO flower-like nanostructure sensor selectivity to ethanol in presence of CO and CH4. Sens. Actuators B, 169 (2012) 67-73

9. S. Shishiyanu, T. Shishiyanu, and O. Lupan. Sensing characteristics of tin-doped ZnO thin films as NO2 gas, Sens. Actuators B, 107 (2005) 379-386.

10. Park, J., Oh, J.Y., Highly-sensitive NO2 detection of ZnO nanorods grown by a sonochemical process. J. Korean Phys. Soc.55, (2009) 1119-1122

11. Pandya, H.J., Chandra, S., Vyas, A.L.: Integration of ZnO nanostructures with MEMS for ethanol sensors. Sens. ActuatorsB, 161, (2012) 923-928

12. Kathwate, L. H., Umadevi, G., Kulal, P. M., Nagaraju, P., Dubal, D. P., Nanjundan, A. K., & Mote, V. D. Ammonia gas sensing properties of Al doped ZnO thin films. Sensors and Actuators A: Physical, 313, (2020). 112193.

13. I. Nkrumah, F.K. Ampong, B. Kwaye-Awuah, R. Kwame Nkkkum, Synthesis and Characterization of ZnO thin films deposited by chemical bath technique. J. Engineering and Technology., 02 (2013) 809-812.

14. X. Hao, J. Ma, D. Zhang, T. Yang, H. Ma, Y. Yang, C. Cheng, J. Huang, Thickness dependence of structural, optical and electrical properties of ZnO:Al films prepared on flexible substrates, Appl. Surf. Sci. 138 (2001) 137-142.

15. J. Lee, K.Ko , B.Park , Electrical and optical properties of ZnO transparent conducting films by the sol–gel method, J. Cryst.Growth, 247 (2003) 119-125.

16. W. Seeber, M. Abou-Helal ,S. Barth, D. Beil , H. Afify, and S. Demian, Transparent semiconducting ZnO:Al thin films prepared by spray pyrolysis, Mater. Sci in Semi. Process. 2 (1999) 45-55.

17. Chan, K.Y., Low, C.Y., Au, B.W.C., Ng, Z.N., Yeoh, M.E., Pang, W.L., Lee, C.L. and Wong, S.K,. Radio frequency magnetron sputter deposited ZnO films doped with Al, Ga and Ti. Materials Research Innovations, 23 (2019) 22-26.

18. Cosme, I., Vázquez-y-Parraguirre, S., Malik, O., Mansurova, S., Carlos, N., Tavira-Fuentes, A., Ramírez, G. and Kudriavtsev, Y., Differences between (103) and (002) X-ray diffraction characteristics of nanostructured AZO films deposited by RF magnetron sputtering. Surface and Coatings Technology, 372 (2019) 442-450.

19. J. Ghosh, R. Ghosh, P. Giri, Tuning the visible photoluminescence in Al doped ZnO thin film and its application in label-free glucose detection, Sensor. Actuator. B Chem. 254 (2018) 681–689

20. Alnajjar, A. A. (2012). ZnO: Al grown by sputtering from two different target sources: a comparison study. Advances in Condensed Matter Physics, 2012, Article ID 682125

21. V. Gokulakrishnan, S. Parthiban, K. Jeganathan, and K. Ramamurthi, Investigations on the structural, optical and electrical properties of Nb-doped SnO2 thin films. J. Mater Sci. 46 (2011) 5553-5558.

22. L. Armelao, M. Fabrizio, S. Gialanella, F. Zordan, Sol–gel synthesis and characterisation of ZnO-based nanosystems, Thin Soli Films 394 (2001) 89-95.

23. B. Benhaoua, A. Rahal, S. Benramache, The structural, optical and electrical properties of nanocrystalline ZnO: Al thin films, Super. Micro. 68 (2014) 38- 47.

24. Q Y. Fu, S. Hao, B.Shen , Preparation and optical-electrical properties of Al-doped ZnO films, Res. Chem. 39 (2013) 527-536.

25. B. D. Cullity, Elements of X-Ray Diffraction, Addison-Wesley, Boston, Mass, USA, 3rd edition, 2001.

26. Viezbicke, Brian D., Patel, Shane, Davis, Benjamin E. & Birnie, Dunbar P. Evaluation of the Tauc Method for Optical Absorption Edge Determination: ZnO Thin Films as a Model System. Physica Status Solidi, B 252 (2015) 1700-1710

27. C. Hui Zhai, R. Jun Zhang. X. Chen, Y. Xiang Zheng, S. You Wang, J. Liu, N. Dai, and L. Yao Chen, Effects of Al doping on the properties of ZnO thin films deposited by atomic layer deposition, J. Nanoscal Res Lett. 11 (2016) 1-15.

28. E. Gungor,and T. Gungor, Influence of aluminum concentration on the electrical and optical properties of ZnO thin films, J. Turkish Chemical Society, 3(3) (2016) 453-462.

29. Y. Liu, Q. Li, H. Shao, Optical and photoluminescent properties of Al-doped zinc oxide thin films by pulse laser deposition, J. Alloys Compd. 485 (2009) 153-163.

30. S. Tewari, and A. Bhattacharjee, Structural, electrical and optical studies on spray-deposited aluminium-doped ZnO thin film, Indi. Acade of Scien. 76 (2011) 153-163.

31. N. Boonyopakorn, R. Rangkupan, and T. Osotchan, Preparation of aluminum doped zinc oxide targets and RF magnetron sputter thin films with various aluminum doping concentrations, J. Sci. Techno. 40 (2018) 824-830.

32. C. Y. Tsay, S. H. Yu, Optolectronic characteristics of UV photodetectors based on sol-gel synthesized GZO semiconductor thin films, J. Alloys Compd. 569 (2014) 145-150.

33. S. Shrestha, R. Ghimire, J. Nakarmi, Y. Sung Kim, C. Yum Park, and J. Hyo Boo, Properties of ZnO: Al Films Prepared by Spin Coating of Aged Precursor Solution. J Bull Korean Chem. Soc. 31 (2010) 112-115.

34. T. Pathak, L. Purohit, Optical property and AC conductivity RF sputtered N-doped ZnO thin film, Advan. Mater. Proce. 2 (1) (2017) 06-09.

35. O. Baka, A. Azizi, S. Velumani, G. Schmerber, Effects of Al concentration on the electrodeposition and properties of transparent Al-doped ZnO thin films, J. Mater Sci: Mater Electron. 25 (2014) 1761-1769.

36. A. Dagamseh, B.Vet, F. Tichelaar, P. Sutta, and M. Zeman, ZnO:Al films prepared by rf magnetron sputtering applied as back reflectors in thin –film silicon solar cells, Thin Soli Films 516 (2008) 7844-7850.

37. B. Mohanty, Y H Jo, D. Yeon, I. Choi, Y. Cho, Stress-induced anomalous shift of optical band gap in ZnO:Al thin films, Appl. Phys. Lett 95 (2009) 62103-62111.

38. B. Nasr, S. Dasgupta, D. Wang, N. Mechau, Electrical resistivity of nanocrystalline Al- doped zinc oxide films as a of Al content and the degree of its segregation at the grain boundaries, J. Appl. Phys, 108 (2010) 103721-6.

39. Ismal R .M, and Podder J, Structural, optical and photocatalysis properties of sol–gel deposited Al-doped ZnO thin films, J. Surf and Int. 16 (2019) 120-126.

40. Tsay C.Y., and Hsu T. W. Comparative studies on ultraviolet light – derived photoresponse properties of ZnO, AZO, and GZO transparent semiconductor thin films. Mater. 10 (2017) 1-12.

41. A. Paola Caricato, A. Luches, and R. Rella, Nanoparticle thin films for Gas Sensors Prepared by Matrix Assisted Pulsed Laser Evaporation, Sensor 9 (2009) 2682-2696

42. H. Hassan, A. Kashyout, I. Morsi, A. Nasser, and A. Raafat, Fabrication and characterization of gas sensor micro-arrays. Sensing and Bio-Sensing Research, 1 (2014) 34-40.

43. M. Chougule, S. Sen,V. Patil, Fabrication of Nanostructured ZnO thin film sensor for NO2 monitoring, Ceram. Int, 38(4) (2011) 2685-2692.

44. V. Galstan, E. Comini, C. Baratto, G. Faglia, and G. Sberveglieri, Nanostructured ZnO chemical gas sensors, Ceram. Int, 41 (2015) 14239- 14244.